Citation: Yi Zhao, Jianchao Zeng, Ying Tan. Two performance indicators assisted infill strategy for expensive many-objective optimization. *Journal of Harbin Institute of Technology (New Series)*. DOI: 10.11916/j.issn.1005-9113.2024081

Two Performance Indicators Assisted Infill Strategy for Expensive Many-Objective Optimization

Yi Zhao[1*], *Jianchao Zeng*[2] *and Ying Tan*[3]

(1. *School of Economics and Management, Taiyuan University of Science and Technology, Taiyuan 030024, Shanxi, China*;
2. *Department of Computer Science and Control Engineering, North University of China, Taiyuan 030051, Shanxi, China*;
3. *Department of Computer Science and Technology, Taiyuan University of Science and Technology, Taiyuan 030024, Shanxi, China*)

Abstract: In recent years, surrogate models derived from genuine data samples have proven to be efficient in addressing optimization challenges that are costly or time-intensive. However, the individuals in the population become indistinguishable as the curse of dimensionality increase in the objective space and the accumulation of surrogate approximated errors. Therefore, in this paper, each objective function is modeled using a radial basis function approach, and the optimal solution set of the surrogate model is located by the multi-objective evolutionary algorithm of strengthened dominance relation. The original objective function values of the true evaluations are converted to two indicator values, and then the surrogate models are set up for the two performance indicators. Finally, an adaptive infill sampling strategy that relies on approximate performance indicators is proposed to assist in selecting individuals for real evaluations from the potential optimal solution set. The algorithm is contrasted against several advanced surrogate-assisted evolutionary algorithms on two suites of test cases, and the experimental findings prove that the approach is competitive in solving expensive many-objective optimization problems.

Keywords: expensive multi-objective optimization problems, infill sample strategy, evolutionary optimization algorithm

CLC number: TP18 **Document code**: A **Article ID**: 1005-9113(2024)00-0000-17

0 Introduction

Multi-objective optimization problems (MOPs), such as the design of a car's cab[1] and pressure vessel design[2], need to optimize two or more conflicting objectives concurrently. The mathematical formula of MOPs is as follows:

$$\min F(\boldsymbol{x}) = (f_1(\boldsymbol{x}), f_2(\boldsymbol{x}), \cdots, f_M(\boldsymbol{x}))$$
$$\text{s.t. } x \in \mathbb{R}^D \quad (1)$$

where $f_i(\boldsymbol{x})(i = 1,2,\cdots,M)$ represents the ith objective of the decision vector $\boldsymbol{x}$. When objective number exceeds 3, they are also described as many-objective optimization problems (MaOPs). Researchers have developed a plethora of evolutionary algorithms aimed at identifying the best solutions of MOPs, which are made up of three types. The first category includes dominance-based multi-objective evolutionary algorithms (MOEAs)[3-4]. The second category features indicator-based MOEAs[5], which adopt an indicator, such as HV[6] or IGD [7], to evaluate the quality of the population. The third of MOEAs is decomposition-based MOEAs, which classify the population into several subgroups[8] or translate the MOPs into multiple single-objective problems[9]. Multi-objective optimization algorithms aim to find a group of convergent and uniformly distributed optimal solutions referred to as the Pareto set (PS) within the decision-making space and the Pareto front (PF) within the space of objectives.

The methods above attained good results on common MOPs. However, they become vestigial on expensive optimization problems, in which a single evaluation of the function can be quite costly[10]. MOEAs involve massive function evaluations (FEs) to approach the optimal set, while there are limited

Received 2024-09-27.
Sponsored by the Scientific and Technological Innovation Programs of Higher Education Institutions in Shanxi (Grant No.2022L294), the Taiyuan University of Science and Technology Scientific Research Initial Funding (Grant No.W2022018, W20242012) and the Foundamental Research Program of Shanxi Province (Grant No.202403021212170).
Corresponding author: Yi Zhao, Ph.D, Lecturer. Email: yizhao1029@126.com.

computational resources in the expensive optimization problems during the optimization process. Surrogates are effective tools for solving expensive optimization problems[11]. Machine learning technologies, such as radial basis function network (RBFN)[12], polynomial regression (PR)[13], and the gaussian process (GP), often referred to as Kriging[14] are commonly used as surrogates. Different surrogates have different advantages[15-16]. For example, Kriging is a probabilistic model which predicts objective values based on the covariance function between the individuals and the true evaluated samples. Moreover, this approach offers an estimated outcome alongside an estimation of the potential variability associated with the objective. Kriging performs well when the decision variable dimension is low, but the high complexity of hyper-parameters makes it difficult to build a Kriging surrogate when the decision variable dimension is greater than 10[17]. RBFN performs well for higher-order nonlinear problems, but it cannot provide approximate uncertainty[18]. In Ref. [19], Zhang proposed to use the heterogeneous database to train objective surrogates and constraint surrogates for disposing of expensive constrained multi-modal problems. In Ref. [20], Li proposed to combine surrogate-assisted evolution optimization and non-model evolutionary optimization to tackle complex expensive optimization problems. Among them, the global surrogate model established by all evaluated samples, the local model trained by a subset of the best solutions, and the local model trained by some newest samples are for forecasting the fitness of individuals. In Ref. [21], Li used the explanation model to assess the critical role of decision variables, and integrated the information into the offspring reproduction. In Ref. [22], Pan used the Kriging model as a surrogate model and proposed an angle penalty distance criterion to filter optimal solutions. More about the methods of surrogate-assisted evolutionary optimization algorithms (SAEAs) can be found in the overview article of Ref. [23].

In the SAEAs, surrogates are designated to replace true function evaluations in three ways. The first way is the regression model-based SAEAs[24-30] which train surrogate models to predict objective functions directly. In Ref. [31], Zhen proposed to utilize a blend of extensive and targeted search tactics to obtain the optimal solution. Furthermore, this methodology leverages a Radial Basis Function (RBF) model for the purpose of predicting the objective function of the candidates in the two stages. In Ref. [32], Wang employed the RBF model and the Kriging model for the approximation of objectives in the global and local search process, respectively. In Ref. [33], Song built GP models tailored for individual objectives in the expensive MOPs by properly using influential points in training samples and adopted the two archive2 method[34] to optimize the population. In Ref. [35], Liu used GP models to estimate each objective and used the true evaluated non-dominated solutions to reset the reference vector adaptively for uneven PF. In Ref. [36], Liu selected Kriging models to estimate each objective and adopted two groups of reference vectors for convergence and diversity searching, respectively. In Ref. [37], Li designed to build an RBFN model for each objective and used a local search strategy grounded in a PF model to exploit the sparse region. The approximate errors will accumulate with the increase of objectives, which increases the difficulties in selecting the authentic Pareto-optimal solutions throughout the course of evolution. The second way is to approximate the indicator function translated from the MOPs with a surrogate model[38]. In Ref. [39], Liu trained the RBFN model to predict the hypervolume indicator (HVI) associated with each solution to assist the environmental selection. The third way is the classification model-based SAEAs which use the surrogates to classify[30,40-45] or predict dominant relationships in the population[46]. In Ref. [44], Wei trained the gradient boosting classifier (GBC) for determining the sorting layer of the individuals in the tiered learning framework of the swarm optimizer (LLSO) and enhance the robustness of SAEAs. In Ref. [47], Pan used RSEA[48] to construct the dominated boundary and selected a feedforward architecture within neural networks (FANNs) to evaluate the precedence among solutions. With the amplification of objectives, the absence of the selection pressure imposed by dominance relation will lead to poor classification performance. Then in Ref. [46], Yuan presented to use deep learning techniques to estimate the Pareto and θ-dominance interactions between solutions. In Ref. [49], Zhang picked two fuzzy classifiers to screen the individuals. One classifier was designed to ascertain the dominance relation and the other was designed to measure the crowdedness of solutions. For the second and third

surrogate-assisted optimization methods, the approximate errors will avoid cumulation with the increase of objectives, but the less output of information in the classification model or indicator model is hard to discriminate the individuals in MOPs.

In the SAEAs, the majority of individuals are evaluated by the surrogates while only a few individuals perform the expensive function evaluations in surrogate-assisted optimization methods. The criterion that picks individuals for real function evaluations is the infill sample strategy. Infill sample strategy is crucial for updating the surrogates and searching for the optimal solutions. There are two classes of individuals considered valid infill samples, one is the individuals with the lowest estimated fitness, while the other consists of those exhibiting the largest uncertainty of the approximated fitness[50]. The individuals possessing the lowest estimated fitness values will be selected for true function evaluations since these individuals can help exploit the promising region and accelerate the convergence of the algorithms[51]. Selecting individuals with the largest uncertainty for real evaluations can augment the prediction precision of the surrogates and facilitate the exploration of sparse regions[17]. It has been shown that the infill strategy which only considers individuals with approximate optimum may give rise to premature convergence or fall into a local optimum[50]. The infill strategy which only considers the prediction uncertainty will consume too many real function evaluations, leading to a slow convergence rate of the algorithm. Therefore, the above two criteria are unsuitable for use alone. The current infill strategies leveraging surrogate models in multi-objective optimization can be sorted into two main types. The first[52-53] of the infill sample strategy is extended by the expected improvement (EI) infill strategy[54] of the expensive single-objective optimization algorithms, which combine the approximate values with the uncertainty as an indicator. In Ref. [53], Zhang used GP models to predict each objective function and these approximate objective functions were used to derive the predictive distribution model for constructing the metric of the infill strategy. In Ref. [55], Wang also selected the GP models to predict the objectives and then used the approximated objective functions to calculate the adaptive acquisition function to pick individuals for the true function evaluations. The second type of the infill strategy uses approximate values and uncertainty as two separate indicators. For the second category of the infill strategy, approximate value and uncertainty are adaptively considered for sampling according to the requirement on convergence or diversity of the population[25,29,56]. In Ref. [26], GP models were used to predict the objectives, and the convergence calculated by the forecasted objective values or the uncertainty of GP models is adaptively preferred for the infill strategy according to the crowding degree of the radial space. In Re. [33], each dimension of objectives is predicted by the pivotal point-insensitive surrogate model and the convergence, diversity, or uncertainty is adaptively considered for the infill strategy according to the predominant demand of convergence, diversity, or uncertainty.

1 Motivation and Contributions

Although the above methods have revealed validity in tackling expensive multi-objective optimization problems (EMOPs), many challenges remain. For the first category of SAEAs, the mistakes from approximations grow more significantly as the objective space expands in dimensionality. The mentioned methods of the infill strategies in SA-MOEAs use the performance indicators which are calculated by the approximated objectives of surrogate models. When the objectives increase, the approximated errors will accumulate. And for the second and third categories of SAEAs, it is difficult to coordinate the convergence and diversity of high-dimensional space with a single performance indicator or classification method. Fig. 1 takes an instance to interpret how the approximated errors induce the performance degradation of the SA-MOEAs. In Fig.1(a), the objective functions of A, B, and C are estimated by the surrogate models, and in Fig.1(b), the objective functions of A, B, and C are assessed through their actual objective functions. In Fig.1(a), suppose we need to choose one individual for the true function evaluations and we utilize the performance indicator that quantifies the Euclidean distance from the candidates to the origin to assess the convergence quality of the individuals. The Euclidean distance of the individuals A, B, and C to the origin is evaluated by the approximated objective functions with 5.10, 2.23, and 4.21, respectively. Considering selecting the individual with the smallest convergence value for the true function evaluations, individual B with the

least Euclidean distance of 2.23 to the origin will be picked. However, the true Euclidean distance of the individuals A, B, and C in Fig.1(b) are 4.71, 5.02, 4.20 where the Euclidean distance of the individual C to the origin is the minimum. In this way, the method of calculating the performance indicators with the approximated objective function values may select individuals with worse convergence performance because of approximate errors accumulating.To further verify the hypothesis in Fig.1, we conducted experimental on the DTLZ1 to DTLZ4 test problems with 10 objectives. The results are shown in Fig. 2. Within Fig.2, we calculate the convergence of Fig.1 employing the fitness values derived from the surrogate model and the actual function evaluation, respectively, and then select individuals for the true evaluation based on these two results. The sum of individuals for each test problem is 20. In Fig.2, it can be seen that the blue bar chart represents the number of individuals whose selection results from the surrogate model and true function evaluations under the same selection criterion are identical, while the orange bar chart represents the number of individuals whose selection results are inconsistent. Fig.2 confirms that the assumption in Fig.1. Thus, to mitigate the negative effect of approximated error accumulation and coordinate convergence and diversity in high-dimensional objective space, this work designs an adaptive infill strategy combining the first and the second way of training surrogate models and proposes the two performance indicators assisted infill strategy for expensive many-objective optimization (TPAEMO). A synthesis of the key contributions of this paper are provided in the subsequent section.

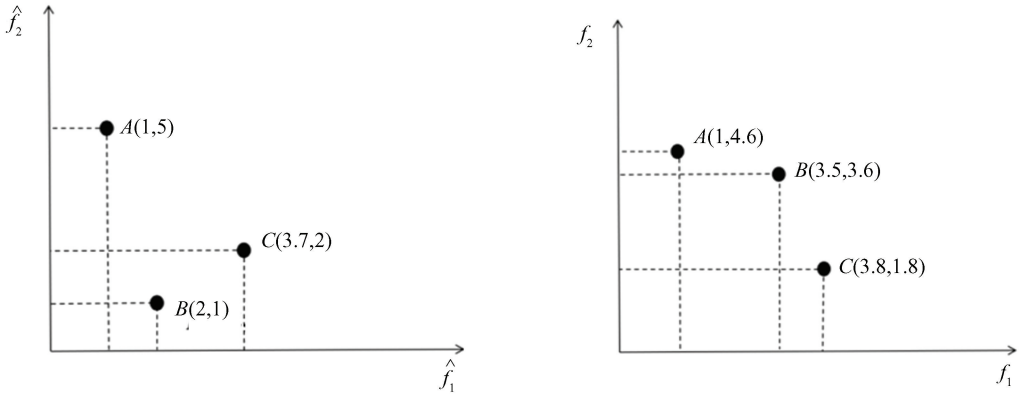

(a) A, B, and C are predicted by the surrogate models (b) A, B, and C are evaluated by the expensive objective functions

Fig.1 An example demonstrating the negative effects that the approximated errors make on the algorithm

1) The surrogate models are established in two ways. The first way is to create a surrogate model for every individual objective, which is used to assist population optimization to coordinate the convergence and diversity within the complex, high-dimensional objective space. The second way is to train the surrogate model for two performance indicators, which is used in the infill criterion and reduces the negative impact of error accumulation.

2) An adaptive infill strategy is designed in which the candidates with good convergence or diversity are picked out for expensive function evaluations based on the level of convergence observed within the group. In this way, it is effective to enhance trade-offs between diversity and convergence.

The subsequent sections of this paper are projected as follows. Section 2 gives concise descriptions of the NSGA-II/SDR algorithm and RBF networks. Section 3 specifically introduce the proposed TPAEMO algorithm. Section 4 displays the outcomes of experiments and parameter analysis. The conclusions and prospect of subsequent research endeavors are given in Section 5.

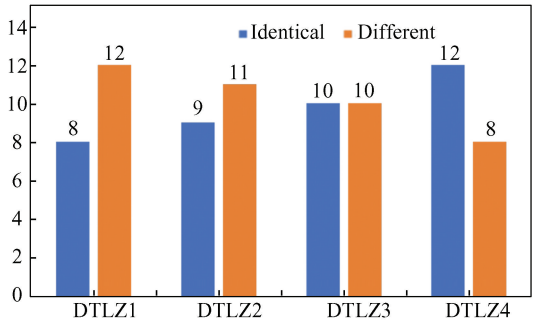

Fig.2 Selection results based on real function evaluation and predicting of surrogate model under the same convergence criterion

2 Preliminaries

2.1 NSGA-II/SDR

NSGA-II[3] is a representative of dominance-based MOEAs that uses the dominance relation to evaluate and compare solutions in multi-objective optimization tasks. When dealing with a higher number of objectives, NSGA-II becomes invalid owing to the deficiency of selection pressure. In Ref. [4], Tian introduced an enhanced version of the dominance relationship known as SDR to bolster the selection pressure of the dominance-based MOEAs for many-objective problems. The standard definition of this enhanced dominance relationship is provided further in the text.

Definition 1 (Strengthened dominance relation). An individual $\boldsymbol{x}$ is said to have an enhanced dominance over another individual $\boldsymbol{y}$ (denoted as $\boldsymbol{x} \prec_{\mathrm{SDR}} \boldsymbol{y}$) if the following conditions are met:

$$\begin{cases} \mathrm{Con}(\boldsymbol{x}) < \mathrm{Con}(\boldsymbol{y}), \theta_{xy} \leqslant \bar{\theta} \\ \mathrm{Con}(\boldsymbol{x}) \cdot \dfrac{\theta_{xy}}{\bar{\theta}} < \mathrm{Con}(\boldsymbol{y}), \ \theta_{xy} > \bar{\theta} \end{cases} \tag{2}$$

where $\mathrm{Con}(\boldsymbol{x}) = \sum_{i=1}^{M} f_i(\boldsymbol{x})$, θ_{xy} represents the angular separation between the individual $\boldsymbol{x}$ and $\boldsymbol{y}$ in the objective space, θ symbolizes a threshold parameter set to the $\lfloor (|P|/2) \rfloor$-th minimum element of

$$\min_{q \in P \setminus p} \theta_{pq} \mid \boldsymbol{p} \in P \tag{3}$$

NSGA-II/SDR embeds the SDR in NSGA-II in which the conventional Pareto dominance relationship is substituted by the SDR. And the NSGA-II/SDR maintains the same overall structure as the standard NSGA-II.

2.2 Radial Basis Function Network

Radial Basis Function Network (RBFN)[15] is a kind of artificial neural network, and it has three fully connected levels which contain an input level, a hidden level and an output level. Given N samples of D decision variables $\boldsymbol{x}_j (j = 1,2,\cdots,N)$ and their objective values $\boldsymbol{y}_j (j = 1,2,\cdots,N)$, the objectives for a novel instance $\boldsymbol{x}$ can be predicted using the following formula:

$$\hat{f}(\boldsymbol{x}) = \sum_{i=1}^{n} \beta_i \varphi(\boldsymbol{x}, \boldsymbol{c}_i) + \eta \tag{4}$$

where $\varphi(\boldsymbol{x}, \boldsymbol{c}_i)$ represents the kernel function used in the hidden level, and $\boldsymbol{c}_i$ is the centroid of the i-th neuron, which is determined through the K-means clustering method. In this paper, we choose the Gaussian kernel as the activation function, which is defined below:

$$\varphi(\boldsymbol{x}, \boldsymbol{c}_i)) = \exp\left(- \frac{\sum_{d=1}^{D} \sqrt{|x^d - c_i^d|^2}}{2\alpha^2} \right) \tag{5}$$

The parameters β_i and η in Eq. (4) need to satisfy the following equation:

$$\sum_{i=1}^{N} \beta_i \varphi_i(x_j, c_i) + \eta = y_j, \ j = 1,2,\cdots,N \tag{6}$$

which can also be expressed in a matrix form below:

$$\begin{bmatrix} \varphi(\boldsymbol{x}_1, \boldsymbol{c}_1) & \varphi(\boldsymbol{x}_1, \boldsymbol{c}_2) & \cdots & \varphi(\boldsymbol{x}_1, \boldsymbol{c}_n) & 1 \\ \varphi(\boldsymbol{x}_2, \boldsymbol{c}_1) & \varphi(\boldsymbol{x}_2, \boldsymbol{c}_2) & \cdots & \varphi(\boldsymbol{x}_2, \boldsymbol{c}_n) & 1 \\ \vdots & \vdots & \ddots & \vdots & \vdots \\ \varphi(\boldsymbol{x}_N, \boldsymbol{c}_1) & \varphi(\boldsymbol{x}_N, \boldsymbol{c}_2) & \cdots & \varphi(\boldsymbol{x}_N, \boldsymbol{c}_n) & 1 \end{bmatrix} \cdot \begin{bmatrix} \beta_1 \\ \vdots \\ \beta_n \\ \eta \end{bmatrix} = \begin{bmatrix} y_1 \\ y_2 \\ \vdots \\ y_N \end{bmatrix} \tag{7}$$

Eq. (7) can alternatively be written as $\boldsymbol{\phi} \cdot \boldsymbol{B} = \boldsymbol{Y}$, and $\boldsymbol{B}^{\mathrm{T}} = [\beta_1, \cdots, \beta_n, \eta]$ can be derived using the method of least squares:

$$\boldsymbol{B} = (\boldsymbol{\phi}^{\mathrm{T}} \cdot \boldsymbol{\phi}) - 1 \cdot \boldsymbol{\phi}^{\mathrm{T}} \cdot \boldsymbol{Y} \tag{8}$$

After obtaining $\boldsymbol{B}$, RBFN makes a prediction as Eq.(4).

3 Proposed Algorithm

3.1 Overall Framework

RBFN with lower complexity in hyper-parameter optimization can better fit the global depiction of the fitness landscape and exhibit better performance for complex problems with high-dimensional and high-order nonlinear aspects[15]. Thus, in this paper, we adopt RBFN models as surrogate models for each objective function and the two performance indicators. Algorithm 1 indicates the pseudocode of the proposed TPAEMO algorithm and the flowchart is displayed in Fig.3. The NSGA-II/SDR severs as the basic optimization framework in TPAEMO. In the main loop, the Latin hypercube sampling (LHS) method is used to create the initial population containing $11D - 1$ individuals. All the individuals in the initial population are calculated by the true objective functions and kept into the archive Arc. Then N individuals with the smallest convergence and biggest diversity are selected from Arc by the environmental selection in NSGA-II/

SDR as the initial population. After that, the N individuals are optimized for several generations. At last, the optimized population is used for the proposed infill strategy, several individuals are recalculated by the true expensive objective functions and then they are added to the database Arc. This process will be executed repeatedly if the true function evaluations is not up to the maximum number and the converged non-dominated optimal solution set will be as the output.

Algorithm 1 The algorithmic pseudocode for TPAEMO

Require: The limit superior in terms of true function evaluations (FE_{max}); population scale N; the count of expensive function evaluations ($FE = 0$)
Ensure: The non-dominated solutions in Arc

1. Take LHS to generate $11D - 1$ individuals, evaluate these individuals, and add them to Arc
2. $FE = FE + 11D - 1$
3. while $FE < FE_{max}$ do
4. Select N individuals in Arc using the environmental selection of NSGA-II/SDR
5. Train an RBF_{obj} surrogate model for each objective using the true sample in Arc
6. Run the optimizer of NSGA-II/SDR assisted by the RBFN models which substitute for the true function evaluation for t generations
7. Select τ individuals, and recalculate them by the true expensive functions
8. (Refer to Algorithm 2)
9. Keep the τ individuals into Arc and update $FE = FE + \tau$
10. end while

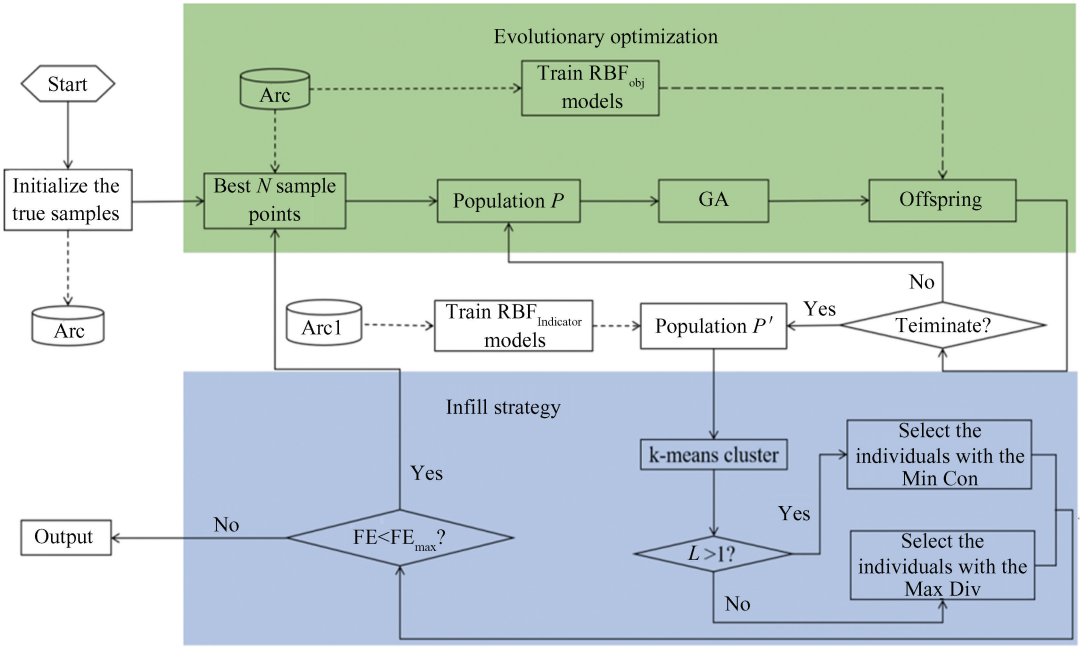

Fig.3 Flowchart of TPAEMO

3.2 Infill Strategy

In SAEAs, general individuals are predicted by the surrogate models and the approximated errors will accumulate with the increase of objectives. To coordinate the convergence and diversity of expensive MaOPs and make the best use of the limited computing resources, an adaptive infill sample strategy is put forward in this article. In the phase of the infill sample strategy, τ individuals will be selected from the optimized population P' for the expensive function evaluations in the TPAEMO. Algorithm 2 displays the pseudocode of the infill sample strategy put forward in TPAEMO. First, all the individuals that have already been evaluated by the expensive functions in the population P' will be identified and deleted. Second, the remaining individuals in P' will be divided into τ clusters using k-means cluster according to their approximated objective functions by RBF_{obj}. Then, the objective function values of the true samples in Arc will be translated to the performance indicators of the convergence and diversity which are defined as

Eq.(9) and Eq.(10):

$$\mathrm{Con}(\boldsymbol{x}) = \sqrt{\sum f(\boldsymbol{x})^2}, (i = 1, \cdots, M) \quad (9)$$

$$\mathrm{Div}(\boldsymbol{x}) = \min_{p \in \mathrm{Arc}, p \neq x} \| F(\boldsymbol{x}), F(\boldsymbol{p}) \| + \frac{1}{\sum_{j=1}^{D+1} 1/d_j(\boldsymbol{x})} \quad (10)$$

where $\| F(\boldsymbol{x}), F(\boldsymbol{p}) \|$ expresses the Euclidean distance between $\boldsymbol{x}$ and $\boldsymbol{p}$ in the objective space, and $d_j(\boldsymbol{x})$ denotes the Euclidean distance between $\boldsymbol{x}$ and the j-th closest data point to $\boldsymbol{x}$ in Arc in the objective space. The true samples and their performance indicators are added to archive Arc1 and the data in Arc1 will be used to train two $\mathrm{RBF}_{\mathrm{indicator}}$ models. After that, the $\mathrm{RBF}_{\mathrm{indicator}}$ models will be adopted to assess the convergence and diversity performance indicators of the population P'. Last, one individual with the minimal convergence performance or the maximum diversity performance approximated by the $\mathrm{RBF}_{\mathrm{indicator}}$ models will be selected from each cluster according to the convergence degree of the population P'. Here, a straightforward method is used to estimate the convergence degree of the population. The non-dominated ranking is used to sort the population P' into several non-dominated levels. If there is more than one non-dominated level which implies that the population shows poor convergence, the individual with the minimal convergence value Con will be selected from each cluster. Otherwise, the individual with the maximum diversity value Div will be chosen from each cluster.

Algorithm 2 The proposed adaptive infill strategy

Require: The population P'; Arc

Ensure: The τ individuals evaluated by the expensive functions

1. Remove all individuals in P' that have been calculated by the true objective functions
2. Use the k-means cluster to classify the remaining population P' into τ subpopulations
3. /* Train two indicator models */
4. Assess the convergence indicator and diversity indicator of the true samples in Arc using Eq.(9) and Eq.(10), respectively, and add their two performance indicator values to Arc1
5. Use the data in Arc1 to train two $\mathrm{RBF}_{\mathrm{indicator}}$ models.
6. (Front_1, Front_2, $\cdots$, Front_L) = Non-dominated-sort (P')
7. Estimate the convergence and diversity value of P' using the surrogate model $\mathrm{RBF}_{\mathrm{indicator}}$
8. /* Select a solution in a subpopulation for expensive function evaluations */
9. if $L > 1$ then
10. Select the individual with the minimal convergence value Con predicted by the $\mathrm{RBF}_{\mathrm{indicator}}$ in each sub-population and reevaluate them by the expensive objective functions.
11. else
12. Select the individual with the maximum diversity value Div predicted by the $\mathrm{RBF}_{\mathrm{indicator}}$ in each sub-population and evaluate them using the expensive functions.
13. end if

4 Experimental Studies

In this section, the performance metric of experiment comparison, and the parameter settings of TPAEMO and other comparison algorithms are presented first. Then, experiments with different values of τ in TPAEMO are conducted to examine the effects of different τ values. After that, the effects of approximate performance indicators are investigated. At last, we contrast TPAEMO with the advanced SA-MOEAs algorithms, including K-RVEA, CSEA, and KTA2. We also compare TPAEMO with NSGA-II/SDR without using the surrogates. All these algorithms are operated on the PlatEMO[57] to obtain the results. The Wilcoxon rank-sum test at a significance of 0.05 is adopted to compare the results of TPAEMO and other algorithms. Symbols "+", "−" and "≈" represent that TPAEMO has achieved better, worse, and similar results with the compared algorithms, respectively. We execute experiments on the test suites of DTLZ[58] and MaF[59] to examine the optimization capability of TPAEMO.

4.1 Performance Metrics

In this paper, we use the performance metric of Inverted Generational Distance (IGD)[60] to compare the optimization capability of different algorithms. IGD uses a group of uniformly distributed reference points sampled along the true Pareto front (PF) to

assess the convergence and diversity of the algorithm. An algorithm performs better on convergence and diversity when it has a lower Inverted Generational Distance (IGD) value. The formula of IGD is showed below:

$$\mathrm{IGD}(P^*,\Omega)=\frac{\sum_{r\in P^*} d(r,\Omega)}{|P^*|} \tag{11}$$

In Eq (11), P^* represents the set of reference points sampled from the true Pareto front, Ω represents the approximate Pareto optimal set achieved by running the algorithm, and $d(r,\Omega)$ represents the smallest Euclidean distance from the point r on the true PF to the individual in Ω.

4.2 Comparison Algorithms and Parameter Configuration

4.2.1 Comparison Algorithms

To test the viability of the proposed algorithm, we contrast TPAEMO against CSEA, K-RVEA, KTA2, and NSGA-II/SDR. A concise description of each comparison algorithm is given below.

(1) CSEA[47]: The method leverages feed-forward neural networks (FNNs) to develop the classification criterion which divides true samples into non-dominated and dominated categories to determine the dominant relationship between newly generated solutions and reference solutions.

(2) K-RVEA[25]: It adopts the Kriging model to estimate each objective function. Then in managing the Kriging models, uncertainty information brought by the Kriging models, the distribution information of the reference vectors, and the position of the individuals are considered for selecting individuals to reevaluate by expensive function.

(3) KTA2[33]: This method constructs one influential point-insensitive model to predict each objective function and consider convergence, diversity, and model accuracy in selecting new individuals for reevaluating according to the foremost demand for convergence, diversity, or uncertainty of the surrogate model.

(4) NSGA-II/SDR[4]: The method is advanced for tackling many-objective optimization problems without surrogate models and an adaptive niching technique of strengthened dominance relation (SDR) is advanced in view of the angle niches between the individuals, where only the best converged individual is installed at the first non-dominated level in each niche.

4.2.2 Parameter Configuration

Parameter configuration of TPAEMO and the compared algorithms are given below:

(1) In our experiments, reproduction operators containing simulated binary crossover and polynomial mutation are employed in all the comparison algorithms to create the offspring solutions. The parameters of reproduction operators are configured as $p_c = 1.0$, $p_m = 1/D$, $\eta_c = 20$, $\eta_m = 20$.

(2) Maximum expensive function evaluations of 300 times serves as the ending condition for all comparison algorithms in this paper.

(3) The population scale of TPAEMO is configured as 50. The initial population scale of the compared algorithms is configured as 50.

(4) The related parameters of the compared algorithms are configured complying with suggestions Refs.[4,25,33,47].

4.3 Sensitivity Analysis of τ

The parameter τ of the number to pick individuals for actual function evaluations may affect the optimization capability of TPAEMO, so we set different values of 1, 3, 5, 8, and 10 for parameter τ to conduct experiments. The mean IGD results of different parameter τ over 20 independent executions on DTLZ1 and DTLZ6 with 10 objectives are shown in Fig 4. From Fig.4, it can be observed that when $\tau = 3$, the mean IGD values of DTLZ1 and DTLZ6 with 10 objectives are minimal. Thus, we set $\tau = 3$.

4.4 Effect of Approximate Performance Indicators

To study the effect of approximate performance indicators predicted by the surrogate models directly, we compare TPAEMO with another variant of the algorithm, named TPAEMO-I, in which the performance indicator values of candidates are calculated by the approximate objectives instead of being predicted by the surrogate model directly. The average IGD results of TPAEMO and TPAEMO-I according to 20 independent executions on DTLZ1-DTLZ7 problems with 3, 4, 6, 8, and 10 objectives are shown in Table 1. The best median result in each row is marked with a gray-colored backdrop. TPAEMO obtained 11 better results and 7 worse results than TPAEMO-I and TPAEMO showed better performance on all objectives of DTLZ5, and high-dimensional objectives of DTLZ2. The results reflect that our TPAEMO shows better performance than TPAEMO-I.

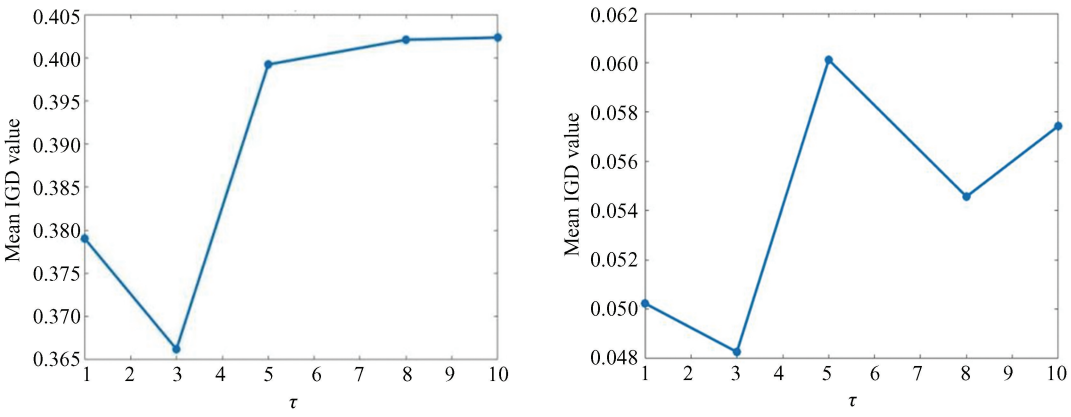

(a) DTLZ1, M=10 (b) DTLZ6, M=10

Fig.4 Mean IGD values attained by different values of τ

Table 1 IGD statistical results attained by TPAEMO-I and TPAEMO for DTLZ1–DTLZ7 with 3, 4, 6, 8, and 10 objectives

Problem	M	TPAEMO-I	TPAEMO
DTLZ1	3	8.7310e+1 (1.90e+1) +	7.4231e+1(1.43e+1)
	4	5.8190e+1 (1.23e+1) ≈	5.4455e+1 (1.61e+1)
	6	2.5358e+1 (6.96e+0) ≈	2.6760e+1 (5.92e+0)
	8	9.3289e+0 (4.07e+0) ≈	7.5787e+0 (3.51e+0)
	10	3.5618e−1 (1.40e−1) ≈	3.6621e−1 (9.24e−2)
DTLZ2	3	5.7747e−2 (1.51e−3) −	8.4222e−2 (1.62e−2)
	4	1.3556e−1 (4.45e−3) −	1.4003e−1 (6.58e−3)
	6	2.8261e−1 (5.51e−3) +	2.7687e−1 (3.45e−3)
	8	3.9200e−1 (1.03e−2) ≈	3.8654e−1 (1.23e−2)
	10	4.9670e−1 (1.62e−2) +	4.8399e−1 (2.07e−2)
DTLZ3	3	2.2357e+2 (4.98e+1) ≈	2.3253e+2 (4.44e+1)
	4	1.7379e+2 (3.26e+1) ≈	1.7264e+2 (2.88e+1)
	6	9.3925e+1 (2.11e+1) +	7.4962e+1 (2.13e+1)
	8	2.9784e+1 (1.25e+1) ≈	2.8447e+1 (1.15e+1)
	10	1.1845e+0 (2.73e−1) ≈	1.4352e+0 (5.16e−1)
DTLZ4	3	3.3055e−1 (1.05e−1) +	2.7979e−1 (8.62e−2)
	4	4.0054e−1 (6.48e−2) ≈	4.1797e−1 (1.29e−1)
	6	4.6784e−1 (2.76e−2) −	5.0070e−1 (5.68e−2)
	8	5.1670e−1 (2.08e−2) ≈	5.1355e−1 (3.00e−2)
	10	5.6173e−1 (1.38e−2) ≈	5.6338e−1 (1.91e−2)
DTLZ5	3	2.6415e−2 (4.68e−3) +	1.0701e−2 (2.39e−3)
	4	2.9298e−2 (3.30e−3) +	1.2641e−2 (1.42e−3)
	6	2.9293e−2 (3.06e−3) +	1.4200e−2 (1.60e−3)
	8	2.0860e−2 (3.96e−3) +	1.3116e−2 (1.89e−3)
	10	9.3267e−3 (8.64e−4) +	6.6032e−3 (4.58e−4)
DTLZ6	3	2.5996e+0 (5.07e−1) ≈	2.8419e+0 (5.47e−1)
	4	2.0375e+0 (3.96e−1) ≈	2.2219e+0 (5.97e−1)
	6	1.2190e+0 (2.19e−1) ≈	1.0972e+0 (4.14e−1)
	8	4.1835e−1 (2.40e−1) ≈	4.4386e−1 (1.77e−1)
	10	4.6037e−2 (1.49e−2) ≈	4.8266e−2 (1.66e−2)
DTLZ7	3	1.7145e−1 (3.06e−2) −	3.2121e−1 (6.96e−2)
	4	2.7639e−1 (4.46e−2) −	4.4570e−1 (6.27e−2)
	6	5.0131e−1 (2.73e−2) −	6.5455e−1 (4.47e−2)
	8	8.0525e−1 (2.69e−2) −	8.8780e−1 (5.46e−2)
	10	1.1569e+0 (4.81e−2) +	1.0814e+0 (2.27e−2)
+/ −/ ≈		11/7/17	

4.5 Effect of the Infill Strategy

To discuss the effect of the infill strategy, we compare TPAEMO with another variant of the algorithm, named TPAEMO-II, in which only the performance indicator of convergence predicted by the surrogate model is employed to choose individuals for expensive function evaluations. The average IGD results of TPAEMO-II and TPAEMO based on 20 independent executions of DTLZ1-DTLZ7 test problems with 3, 4, 6, 8, and 10 objectives are shown in Table 2 TPAEMO obtained 9/35 better results than TPAEMO-II and 0/35 worse results than TPAEMO-II which indicates that the infill strategy used in TPAEMO is more effective than that in TPAEMO-II. TPAEMO performed better than TPAEMO mainly on DTLZ2 which showed the performance indicator of diversity used in TPAEMO is effective.

Table 2 IGD statistical results attained by TPAEMO-II and TPAEMO for DTLZ1–DTLZ7 with 3, 4, 6, 8, and 10 objectives

Problem	*M*	TPAEMO-II	TPAEMO
DTLZ1	3	8.1097e+1 (1.39e+1) ≈	7.4231e+1 (1.43e+1)
	4	5.5345e+1 (1.70e+1) ≈	5.4455e+1 (1.61e+1)
	6	2.7662e+1 (6.01e+0) ≈	2.6760e+1 (5.92e+0)
	8	8.7150e+0 (4.11e+0) ≈	7.5787e+0 (3.51e+0)
	10	4.0548e−1 (1.23e−1) ≈	3.6621e−1 (9.24e−2)
DTLZ2	3	1.1222e−1 (2.01e−2) +	8.4222e−2 (1.62e−2)
	4	1.9705e−1 (2.33e−2) +	1.4003e−1 (6.58e−3)
	6	3.7566e−1 (3.78e−2) +	2.7687e−1 (3.45e−3)
	8	5.5145e−1 (3.82e−2) +	3.8654e−1 (1.23e−2)
	10	6.0336e−1 (4.79e−2) +	4.8399e−1 (2.07e−2)
DTLZ3	3	2.2325e+2 (4.98e+1) ≈	2.3253e+2 (4.44e+1)
	4	1.6697e+2 (4.33e+1) ≈	1.7264e+2 (2.88e+1)
	6	7.8945e+1 (2.70e+1) ≈	7.4962e+1 (2.13e+1)
	8	2.9895e+1 (1.09e+1) ≈	2.8447e+1 (1.15e+1)
	10	1.2707e+0 (3.63e−1) ≈	1.4352e+0 (5.16e−1)
DTLZ4	3	4.6745e−1 (2.55e−1) +	2.7979e−1 (8.62e−2)
	4	4.0139e−1 (8.52e−2) ≈	4.1797e−1 (1.29e−1)
	6	5.4220e−1 (8.91e−2) ≈	5.0070e−1 (5.68e−2)
	8	5.1293e−1 (3.74e−2) ≈	5.1355e−1 (3.00e−2)
	10	5.7202e−1 (2.37e−2) ≈	5.6338e−1 (1.91e−2)
DTLZ5	3	1.0619e−2 (1.47e−3) ≈	1.0701e−2 (2.39e−3)
	4	1.3465e−2 (1.84e−3) ≈	1.2641e−2 (1.42e−3)
	6	1.4554e−2 (2.37e−3) ≈	1.4200e−2 (1.60e−3)
	8	1.2194e−2 (1.61e−3) ≈	1.3116e−2 (1.89e−3)
	10	6.7119e−3 (5.76e−4) ≈	6.6032e−3 (4.58e−4)
DTLZ6	3	2.5807e+0 (5.66e−1) ≈	2.8419e+0 (5.47e−1)
	4	2.3335e+0 (4.66e−1) ≈	2.2219e+0 (5.97e−1)
	6	1.2033e+0 (3.91e−1) ≈	1.0972e+0 (4.14e−1)
	8	5.4745e−1 (2.72e−1) ≈	4.4386e−1 (1.77e−1)
	10	4.8432e−2 (1.58e−2) ≈	4.8266e−2 (1.66e−2)
DTLZ7	3	3.3904e−1 (8.98e−2) ≈	3.2121e−1 (6.96e−2)
	4	4.6441e−1 (7.84e−2) ≈	4.4570e−1 (6.27e−2)
	6	6.9609e−1 (4.79e−2) +	6.5455e−1 (4.47e−2)
	8	1.0470e+0 (1.03e−1) +	8.8780e−1 (5.46e−2)
	10	1.3239e+0 (6.13e−2) +	1.0814e+0 (2.27e−2)
+/ − /	≈	9/0/26	

4.6 Comparison over Other Algorithms

We test the optimization capability of TPAEMO on DTLZ1−DTLZ7 problems with 3, 4, 6, 8, and 10 objectives and MaF1−MaF7 problems with 3, 5, and 10 objectives. Regarding all of the test cases, the dimension of the decision variable is 10.

1) Results on DTLZ benchmarks: the IGD scores attained by the five compared algorithms across 20 separate executions on DTLZ1 through DTLZ7 are collected in Table 3, where the best median result in each row is marked with a gray-colored backdrop. From Table 3, it can be seen that TPAEMO obtained 25 better results and 2 worse results than NSGA-II/SDR within a group of 35 test examples, which indicates that TPAEMO is more efficient

than NSGA-II/SDR which has no surrogate model to participate in tackling the computationally expensive many-objective test problems. Table 3 reveals the following results that TPAEMO obtained 15 best median results within the 35 test instances, KTA2 ranked second with the 10 most successful results, CSEA ranked third with 5 superior results, and K-RVEA ranked fourth with 5 finest results.

Table 3 IGD statistical results attained by CSEA, K-RVEA, KTA2, NSGA-II/SDR, and TPAEMO for DTLZ1–DTLZ7 with 3, 4, 6, 8, and 10 objectives

Problem	M	CSEA	K-RVEA	KTA2	NSGAIISDR	TPAEMO
DTLZ1	3	5.9534e+1 (1.25e+1)−	8.1481e+1 (1.80e+1) ≈	4.8197e+1 (1.41e+1)−	8.3781e+1 (2.17e+1) ≈	7.4231e+1 (1.43e+1)
	4	4.0939e+1 (1.13e+1) −	5.4846e+1 (1.90e+1) ≈	3.6212e+1 (9.26e+0) −	5.7256e+1 (1.35e+1) ≈	5.4455e+1 (1.61e+1)
	6	1.5112e+1 (4.53e+0) −	2.6899e+1 (1.04e+1) ≈	1.4708e+1 (5.22e+0) −	2.2069e+1 (6.65e+0) −	2.6760e+1 (5.92e+0)
	8	4.2113e+0 (2.20e+0)−	7.9373e+0 (2.95e+0) ≈	5.8784e+0 (2.25e+0) ≈	5.4764e+0 (2.52e+0) ≈	7.5787e+0 (3.51e+0)
	10	2.8425e−1 (8.21e−2)−	3.1756e−1 (9.10e−2) ≈	3.2361e−1 (8.38e−2) ≈	3.9623e−1 (1.53e−1) ≈	3.6621e−1 (9.24e−2)
DTLZ2	3	2.4099e−1 (3.53e−2) +	1.2034e−1 (1.85e−2) +	6.4847e−2 (4.08e−3)−	2.8189e−1 (2.97e−2) +	8.4222e−2 (1.62e−2)
	4	3.2764e−1 (3.60e−2) +	2.2083e−1 (1.84e−2) +	1.4633e−1 (5.96e−3) +	3.4013e−1 (2.87e−2) +	1.4003e−1 (6.58e−3)
	6	4.9143e−1 (3.25e−2) +	3.4909e−1 (1.69e−2) +	2.9517e−1 (1.16e−2) +	4.4130e−1 (2.91e−2) +	2.7687e−1 (3.45e−3)
	8	6.2001e−1 (3.29e−2) +	4.3836e−1 (1.79e−2) +	4.0115e−1 (8.47e−3) +	6.0370e−1 (7.50e−2) +	3.8654e−1 (1.23e−2)
	10	6.7637e−1 (2.34e−2) +	5.2403e−1 (2.69e−2) +	4.3593e−1 (7.90e−3)−	7.1299e−1 (4.49e−2) +	4.8399e−1 (2.07e−2)
DTLZ3	3	1.5569e+2 (3.37e+1)−	1.5601e+2 (7.12e+1)−	1.2253e+2 (4.87e+1)−	2.4284e+2 (5.11e+1) ≈	2.3253e+2 (4.44e+1)
	4	1.1189e+2 (3.87e+1)−	1.3986e+2 (4.69e+1)−	1.0640e+2 (3.22e+1)−	1.8361e+2 (4.10e+1) ≈	1.7264e+2 (2.88e+1)
	6	5.9675e+1 (1.58e+1)−	6.9305e+1 (2.11e+1) ≈	5.0164e+1 (1.57e+1)−	8.5978e+1 (2.82e+1) ≈	7.4962e+1 (2.13e+1)
	8	1.4747e+1 (5.19e+0)−	1.9684e+1 (9.51e+0)−	1.6355e+1 (1.02e+1)−	1.9838e+1 (8.40e+0)−	2.8447e+1 (1.15e+1)
	10	9.5269e−1 (1.24e−1)−	8.7563e−1 (3.83e−1)−	1.1251e+0 (3.67e−1)−	1.3089e+0 (4.34e−1) ≈	1.4352e+0 (5.16e−1)
DTLZ4	3	4.6070e−1 (1.75e−1) +	3.0591e−1 (9.14e−2) ≈	3.4258e−1 (2.57e−1) ≈	8.1398e−1 (1.56e−1) +	2.7979e−1 (8.62e−2)
	4	3.3243e−1 (5.81e−2)−	3.9298e−1 (9.08e−2) ≈	4.1919e−1 (1.41e−1) ≈	9.2176e−1 (1.23e−1) +	4.1797e−1 (1.29e−1)
	6	4.7341e−1 (4.64e−2) ≈	5.1398e−1 (6.24e−2) ≈	5.5366e−1 (1.02e−1) ≈	9.6216e−1 (1.53e−1) +	5.0070e−1 (5.68e−2)
	8	5.7000e−1 (3.27e−2) +	5.6520e−1 (3.47e−2) +	5.8830e−1 (8.09e−2) +	9.9062e−1 (1.15e−1) +	5.1355e−1 (3.00e−2)
	10	6.4429e−1 (3.06e−2) +	6.6835e−1 (3.05e−2) +	5.9165e−1 (4.09e−2) +	7.9606e−1 (1.32e−1) +	5.6338e−1 (1.91e−2)
DTLZ5	3	1.2398e−1 (3.43e−2) +	8.0264e−2 (1.51e−2) +	1.0771e−2 (2.88e−3) ≈	2.1040e−1 (3.00e−2) +	1.0701e−2 (2.39e−3)
	4	1.2978e−1 (2.21e−2) +	4.6540e−2 (9.45e−3) +	5.5606e−2 (1.32e−2) +	1.9175e−1 (3.73e−2) +	1.2641e−2 (1.42e−3)
	6	8.0606e−2 (2.01e−2) +	3.7516e−2 (1.33e−2) +	6.7885e−2 (1.91e−2) +	1.4790e−1 (2.44e−2) +	1.4200e−2 (1.60e−3)
	8	4.6715e−2 (8.53e−3) +	2.5423e−2 (5.40e−3) +	6.3113e−2 (1.37e−2) +	1.2903e−1 (2.66e−2) +	1.3116e−2 (1.89e−3)
	10	1.4326e−2 (1.36e−3) +	1.2634e−2 (2.00e−3) +	1.9667e−2 (3.37e−3) +	8.0234e−2 (8.00e−3) +	6.6032e−3 (4.58e−4)
DTLZ6	3	5.8812e+0 (4.59e−1) +	2.8777e+0 (4.40e−1) ≈	1.7679e+0 (5.03e−1)−	5.8587e+0 (3.15e−1) +	2.8419e+0 (5.47e−1)
	4	5.0638e+0 (4.86e−1) +	2.0288e+0 (3.46e−1) ≈	1.8498e+0 (5.75e−1) ≈	5.0287e+0 (3.86e−1) +	2.2219e+0 (5.97e−1)
	6	3.0018e+0 (4.85e−1) +	1.1790e+0 (3.58e−1) ≈	1.4152e+0 (5.07e−1) +	3.5228e+0 (2.43e−1) +	1.0972e+0 (4.14e−1)
	8	1.2243e+0 (4.47e−1) +	5.2976e−1 (1.83e−1) ≈	9.9739e−1 (4.33e−1) +	2.0436e+0 (3.21e−1) +	4.4386e−1 (1.77e−1)
	10	1.9395e−1 (2.37e−1) +	8.3187e−2 (3.85e−2) +	9.6057e−2 (3.86e−2) +	4.8988e−1 (2.45e−1) +	4.8266e−2 (1.66e−2)
DTLZ7	3	1.4927e+0 (4.91e−1) +	1.0389e−1 (8.38e−3)−	4.2266e−1 (2.78e−1) ≈	4.4702e+0 (1.29e+0) +	3.2121e−1 (6.96e−2)
	4	2.8625e+0 (9.00e−1) +	2.8130e−1 (6.42e−2)−	6.1968e−1 (3.05e−1) ≈	5.9308e+0 (1.27e+0) +	4.4570e−1 (6.27e−2)
	6	8.5548e+0 (2.43e+0) +	5.5049e−1 (6.17e−2)−	6.7099e−1 (2.09e−1) ≈	5.4100e+0 (1.58e+0) +	6.5455e−1 (4.47e−2)
	8	8.2860e+0 (2.97e+0) +	8.9132e−1 (7.45e−2) ≈	1.0837e+0 (3.42e−1) ≈	3.5206e+0 (1.26e+0) +	8.8780e−1 (5.46e−2)
	10	2.0119e+0 (2.98e−1) +	1.0186e+0 (2.21e−2)−	1.3457e+0 (3.41e−1) +	1.8389e+0 (6.44e−1) +	1.0814e+0 (2.27e−2)
+/−/≈		23/11/1	13/8/14	13/11/11	25/2/8	

TPAEMO performed the best among other comparison algorithms in the context of DTLZ2, DTLZ4, DTLZ5, and DTLZ6, and performed worse than other comparison algorithms on DTLZ1, DTLZ3, and DTLZ7. For DTLZ1 and DTLZ3, they contain a lot of locally non-dominated solutions that are hard to converge. KTA2 performed best on DTLZ1 and DTLZ3, and CSEA ranked second. The call for convergence frequently emerges in the optimization of local Pareto optimal problems, so KTA2 frequently selects well-converged solutions in the sampling strategy. CSEA takes convergence into consideration so CSEA selected potentially better-converged solutions for expensive evaluations. K-RVEA used a group of well-distributed reference vectors to navigate the search, so K-RVEA obtained a set of uniformly distributed solutions. TPAEMO tries to coordinate convergence and diversity and when facing multi-local optimal solutions, the diversity of infill strategy is frequently used.

For DTLZ2, TPAEMO performed the best, followed by KTA2. This might be due to the infill sampling strategies used in TPAEMO and KTA2 which try to support the co-development of convergence and diversity. The parallel axis plot depicting non-dominated solutions in the run with the best IGD values for K-RVEA, CSEA, KTA2 NSGA-II/SDR, and TPAEMO for 8-objective DTLZ2 is displayed in Fig.5. We can discover from Fig.5 that the upper bound of objectives for the non-dominated solution set acquired by TPAEMO exhibits lower values than the compared algorithms and the non-dominated solutions of TPAEMO possess a more intense distribution than NSGA-II/SDR. This means that TPAEMO exhibits superior results regarding convergence and diversity compared to the algorithms K-RVEA, CSEA, KTA2 and NSGA-II/SDR, and TPAEMO can coordinate convergence and diversity commendably. Since DTLZ4 is a biased multi-objective optimization problem, it is difficult for the algorithms to ensure diversity. As indicated in Table 3, for DTLZ4, TPAEMO performed best. To conduct an in-depth analysis of different algorithms' performance on DTLZ4, the non-dominated solutions of the run with the best IGD values for CSEA, NSGA-II/SDR, K-RVEA, TPAEMO, and KTA2 for DTLZ4 are displayed in Fig.6. From Fig.6 we can observe that the Pareto-front solutions generated by TPAEMO are the closest to the true PF of DTLZ4, followed by KTA2. And the diversity of TPAEMO is better than KTA2 on DTLZ4. Although the diversity of K-RVEA on DTLZ4 is the best owing to the uniformly distributed reference vectors used in K-RVEA, the Pareto-front solutions generated by K-RVEA have a farther distance to the true PF than TPAEMO and KTA2. For NSGA-II/SDR, it maintained the worst diversity.

DTLZ5 and DTLZ6 are degenerate test problems, and TPAEMO performed best on these two kinds of problems. The majority of reference vectors used in K-RVEA are empty on the degenerate problems which makes it not easy to approach to the true Pareto front fast. For DTLZ7 with a disconnected Pareto front, K-RVEA performed best, followed by TPAEMO. Although TPAEMO do not perform the best on DTLZ1, DTLZ3, and DTLZ7, it still exhibits a comparative advantage in contrast with the other four algorithms.

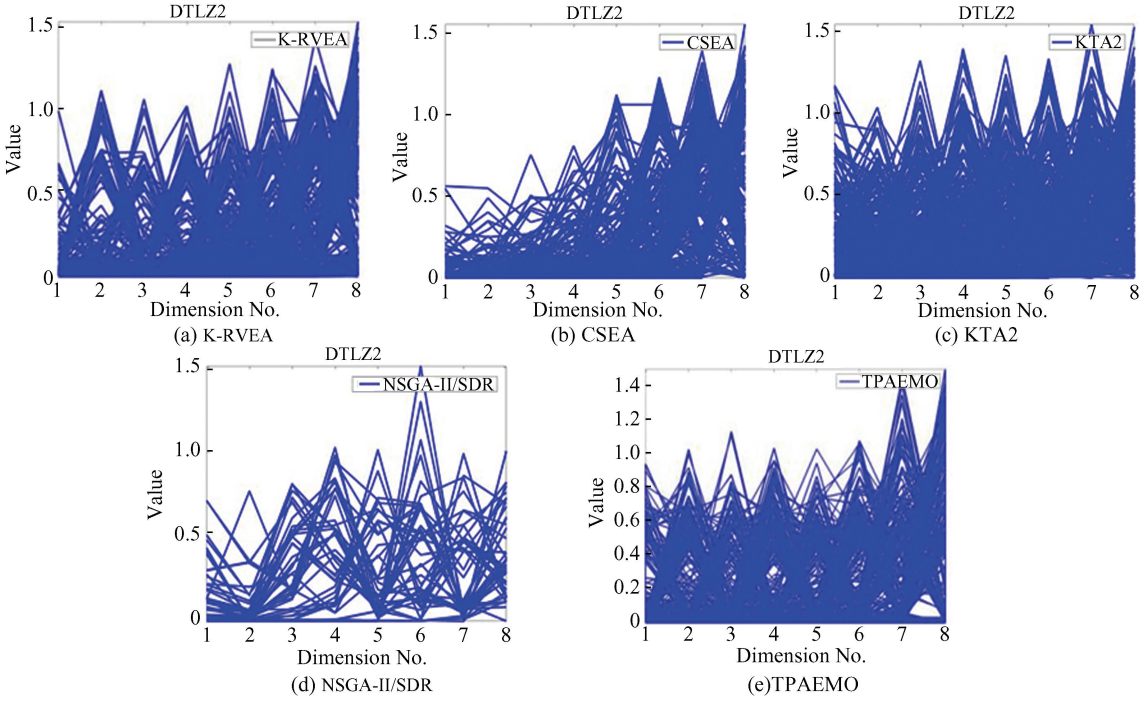

Fig.5 The parallel coordinates graph for the Pareto-optimal solutions attained by K-RVEA, CSEA, KTA2, NSGA-II/SDR, and TPAEMO in the executions with the best IGD value on 8-objective DTLZ2

2) Results on MaF benchmarks: additionally, we compare the performance of TPAEMO with other algorithms on MaF test problems and the results of IGD values attained by the four algorithms under comparison over 20 independent executions on MaF1 to MaF7 are collected in Table 4, where the best median result in each row is marked with a gray background. Among these problems[59], MaF1 with an inverted PF is translated from

DTLZ1, MaF2 is the transformed version of DTLZ2. MaF3 and MaF4 are translated from DTLZ3. MaF5, MaF6, and MaF7 are translated from DTLZ4, DTLZ5 and DTLZ7 respectively.

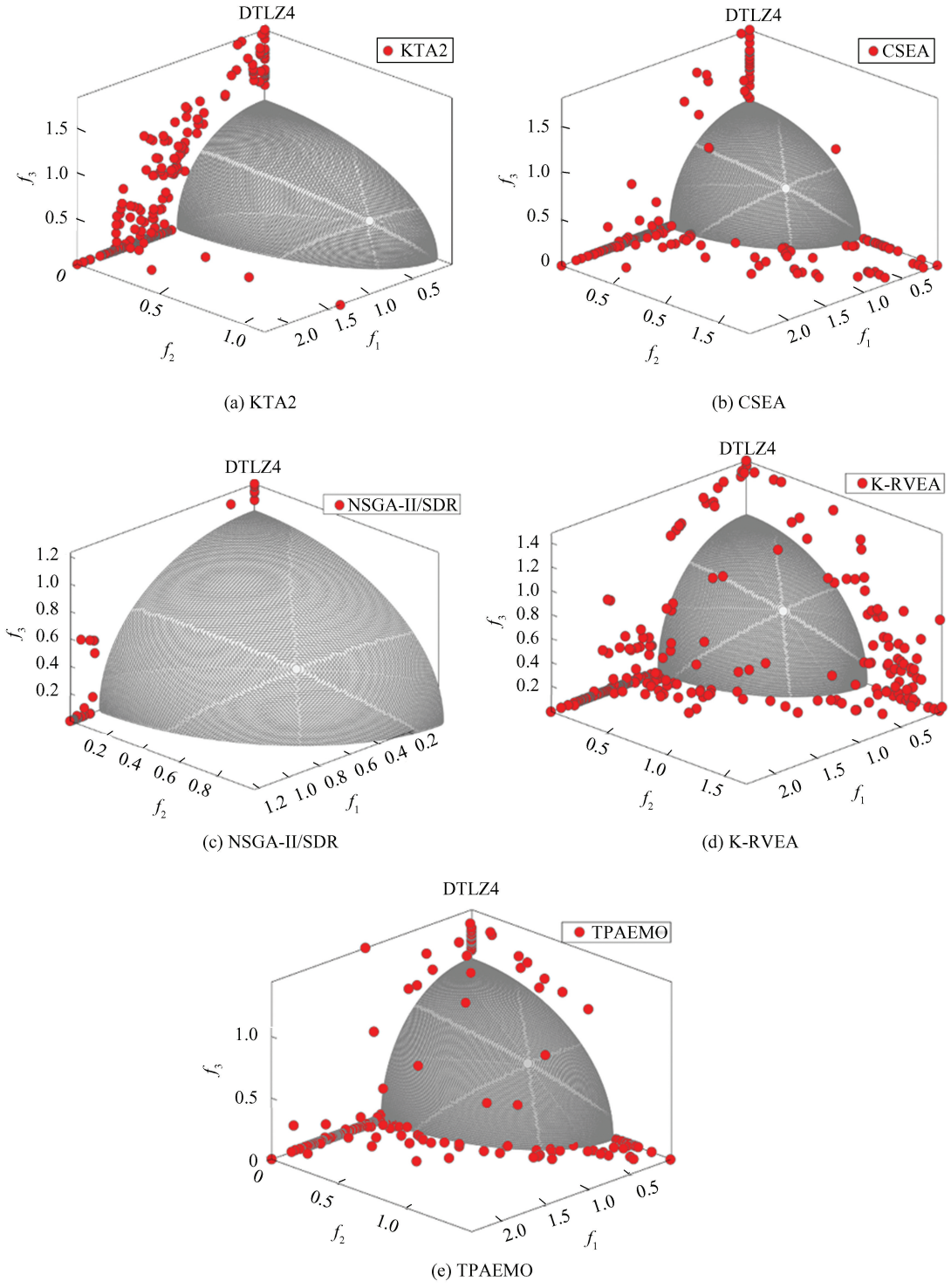

(a) KTA2 (b) CSEA

(c) NSGA-II/SDR (d) K-RVEA

(e) TPAEMO

Fig. 6 Pareto-optimal solutions attained with CSEA, NSGA-II/SDR, K-RVEA, TPAEMO, and KTA2 of the executions with the best IGD value for three-objective DTLZ4

From Table 4, we can discover that TPAEMO attained 13 superior outcomes than CSEA and 10 superior outcomes than K-RVEA among 21 test problems. Compared with NSGA-II/SDR, TPAEMO obtained 16 better results and 0 worse results which indicates our method is more valid than the compared algorithms.

Table 4 IGD statistical results attained by CSEA, K-RVEA, NSGA-II/SDR, and TPAEMO for MaF1– MaF7 with 3, 5, and 10 objectives

Problem	M	CSEA	K-RVEA	NSGA-II/SDR	TPAEMO
MaF1	3	1.7663e−1 (2.58e−2) +	5.6797e−2 (4.55e−3)−	2.9460e−1 (3.65e−2) +	1.1768e−1 (2.54e−2)
	5	2.1933e−1 (1.83e−2) +	1.4934e−1 (2.43e−2) +	3.4144e−1 (4.02e−2) +	1.3397e−1 (1.10e−2)
	10	2.6136e−1 (1.30e−2)−	4.1587e−1 (2.02e−2) +	3.5774e−1 (2.51e−2) +	2.8788e−1 (2.01e−2)
MaF2	3	5.1787e−2 (2.55e−3) +	3.8116e−2 (1.33e−3) +	5.6111e−2 (2.66e−3) +	3.0231e−2 (1.88e−3)
	5	9.9174e−2 (2.05e−3) +	9.0676e−2 (1.87e−3) +	1.3037e−1 (4.56e−3) +	8.8343e−2 (1.37e−3)
	10	3.3337e−1 (1.75e−2) +	3.0575e−1 (2.56e−2) +	4.3777e−1 (5.99e−2) +	2.5027e−1 (2.37e−2)
MaF3	3	2.2830e+5 (2.27e+5) ≈	5.7236e+5 (2.75e+5) +	1.3020e+5 (6.83e+4) ≈	1.4280e+5 (4.75e+4)
	5	1.1625e+5 (1.01e+5) +	2.2184e+5 (1.19e+5) +	3.3353e+4 (2.05e+4) ≈	3.2992e+4 (1.12e+4)
	10	9.9204e−1 (1.59e+0)−	3.6928e+0 (4.82e+0) +	1.7695e+0 (1.42e+0) ≈	1.2699e+0 (1.23e+0)
MaF4	3	5.4813e+2 (1.29e+2) −	8.1020e+2 (2.73e+2) ≈	9.7838e+2 (2.10e+2) +	7.6240e+2 (1.86e+2)
	5	1.2612e+3 (3.83e+2) −	1.2016e+3 (3.77e+2) −	1.8689e+3 (5.52e+2) ≈	1.7645e+3 (3.94e+2)
	10	2.1824e+2 (9.47e+1) −	2.6880e+2 (8.44e+1) −	3.7203e+2 (2.72e+2) ≈	4.0018e+2 (1.75e+2)
MaF5	3	1.5802e+0 (5.22e−1) ≈	1.3278e+0 (3.67e−1) ≈	3.0502e+0 (1.21e+0) +	1.5066e+0 (3.36e−1)
	5	4.5112e+0 (1.00e+0)−	4.5402e+0 (5.28e−1)−	1.1297e+1 (5.09e+0) +	6.0729e+0 (8.40e−1)
	10	1.1241e+2 (2.08e+1) +	1.0870e+2 (2.27e+1) ≈	2.1780e+2 (7.52e+1) +	9.6780e+1 (2.11e+1)
MaF6	3	3.5913e+0 (2.07e+0) +	9.1551e−1 (4.61e−1) +	1.1417e+1 (4.53e+0) +	2.3983e−2 (6.69e−3)
	5	1.5907e+0 (6.19e−1) +	3.2016e−1 (1.07e−1) +	4.0576e+0 (2.35e+0) +	5.5768e−2 (1.45e−2)
	10	2.3343e−2 (7.59e−3) +	1.8401e−2 (8.91e−3) ≈	6.7844e−2 (3.47e−2) +	1.6299e−2 (4.36e−3)
MaF7	3	1.4357e+0 (7.20e−1) +	1.0756e−1 (1.11e−2) −	4.4204e+0 (9.04e−1) +	3.5931e−1 (7.54e−2)
	5	5.1999e+0 (1.41e+0) +	4.5211e−1 (1.05e−1) −	6.0043e+0 (1.62e+0) +	5.1403e−1 (5.16e−2)
	10	1.9913e+0 (2.59e−1) +	1.0302e+0 (3.80e−2) −	1.8785e+0 (5.34e−1) +	1.0953e+0 (3.18e−2)
+/−/≈		13/6/2	10/7/4	16/0/5	

5 Conclusions

In this work, a new surrogate-assisted many-objective evolutionary optimization algorithm for tackling expensive many-objective optimization problems is proposed, in which the surrogate models are constructed to estimate the objective functions and the performance indicators of convergence and diversity. In the surrogate-assisted optimization phase, the objective functions approximated by the surrogate models are used for searching globally optimal areas. Then, to avoid the approximated errors accumulating, the approximated objectives coordinate with approximated performance indicators of convergence and diversity are used in the phase of selecting individuals for true objective function evaluations. In addition, the approximated performance indicators of convergence and diversity are adaptively considered in the infill strategy according to the distribution of the population.

To examine the effectiveness of TPAEMO, two sets of test problems are adopted to contrast the proposed method with four algorithms including CSEA, K-RVEA KTA2, and NSGA-II/SDR. The results of the experiments confirm that TPAEMO performs relatively better and converges more rapidly than the compared three most advanced surrogate-assisted multi-objective optimization algorithms and one MOEA algorithm without surrogate models.

Although TPAEMO has shown good performance in dealing with EMOPs, its performance in tackling disconnected expensive many-objective optimization problems must still be improved. In the future work, we may explore growing neural gas network (iGNG)[35] or distribution information of the PFs[61] in the decision and objective space for model management to further improve the performance of handling EMOPs problems.

References

[1] Deb K, Jain H. An evolutionary many-objective optimization algorithm using reference-point-based nondominated sorting approach, partI: Solving problems with box constraints. IEEE Transactions on Evolutionary Computation, 2014, 18(4): 577−601.

DOI: 10.1109/TEVC.2013.2281535.

[2] Kannan B K, Kramer S N. An Augmented lagrange multiplier based method for mixed integer discrete continuous optimization and its applications to mechanical design. Journal of Mechanical Design, 1994, 116(2): 405-411. DOI: 10.1115/1.2919393.

[3] Deb K, Pratap A, Agarwal S, et al. A fast and elitist multiobjective genetic algorithm: NSGA-II. IEEE Transactions on Evolutionary Computation, 2002, 6(2): 182-197. DOI: 10.1109/4235.996017.

[4] Tian Y, Cheng R, Zhang X, et al. A strengthened dominance relation con- sidering convergence and diversity for evolutionary many-objective optimization. IEEE Transactions on Evolutionary Computation, 2019, 23(2): 331-345. DOI: 10.1109/TEVC.2018.2866854.

[5] Tian Y, Cheng R, Zhang X, et al. An indicator-based multiobjective evo-lutionary algorithm with reference point adaptation for better versatility. IEEE Transactions on Evolutionary Computation, 2018, 22(4): 609-622. DOI: 10.1109/TEVC.2017.2749619.

[6] Bader J, Zitzler E. Hype: An algorithm for fast hypervolume-based many-objective optimization. Evol Comput, 2011, 19(1): 45-76. DOI: 10.1162/EVCO_a_00009.

[7] Sun Y, Yen G G, Yi Z. IGD indicator-based evolutionary algorithm for many-objective optimization problems. IEEE Transactions on Evolutionary Computation, 2019, 23(2): 173-187. DOI: 10.1109/TEVC.2018.2791283.

[8] Cheng R, Jin Y, Olhofer M, et al. A reference vector guided evolutionary algorithm for many-objective optimization. IEEE Trans Evol Comput, 2016, 20(5): 773-791. DOI: 10.1109/TEVC.2016.2519378.

[9] Zhang Q, Li H. MOEA/D: A multiobjective evolutionary algorithm based on decomposition. IEEE Transactions on Evolutionary Computation, 2007, 11(6): 712-731.

[10] Pan J S, Liu N, Chu S C, et al. An efficient surrogate-assisted hybrid optimization algorithm for expensive optimization problems. Information Sciences, 2021, 561: 304-325. DOI: 10.1016/j.ins.2020.11.056.

[11] Jin Y, Wang H, Chugh T, et al. Data-driven evolutionary optimization: An overview and case studies. IEEE Transactions on Evolutionary Computation, 2019, 23(3): 442-458. DOI: 10.1109/TEVC.2018.2869001.

[12] Cai X, Qiu H, Gao L, et al. An efficient surrogate-assisted particle swarm optimization algorithm for high-dimensional expensive problems. Knowledge-Based Systems, 2019, 184: 104901. DOI: 10.1016/j.knosys.2019.104901.

[13] Krithikaa M, Mallipeddi R. Differential evolution with an ensemble of low-quality surrogates for expensive optimization problems. In: 2016 IEEE Congress on Evolutionary Computation (CEC). Piscataway: IEEE, 2016: 78-85. DOI: 10.1109/CEC.2016.7743781.

[14] Buche D, Schraudolph N, Koumoutsakos P. Accelerating evolutionary algorithms with gaussian process fitness function models. IEEE Transactions on Systems, Man, and Cybernetics, Part C (Applications and Reviews), 2005, 35(2): 183-194. DOI: 10.1109/TSMCC.2004.841917.

[15] Liu Z, Wang H, Jin Y. Performance indicator-based adaptive model selection for offline data-driven multiobjective evolutionary optimization. IEEE Transactions on Cybernetics, 2023, 53(10): 6263-6276. DOI: 10.1109/TCYB.2022.3170344.

[16] Zhen H, Gong W, Wang L. Offline data-driven evolutionary optimization based on model selection. Swarm and Evolutionary Computation, 2022, 71: 101080. DOI: 10.1016/j.swevo.2022.101080.

[17] Tian J, Tan Y, Zeng J, et al, Multiobjective infill criterion driven gaus-sian process-assisted particle swarm optimization of high-dimensional expensive problems. IEEE Transactions on Evolutionary Computation, 2019, 23(3): 459-472. DOI: 10.1109/TEVC.2018.2869247.

[18] Zhao Y, Zhao J, Zeng J, et al. A two-stage infill strategy and surrogate-ensemble assisted expensive many-objective optimization. Complex & Intelligent Systems, 2022, 8: 5047-5063. DOI: 10.1007/s40747-022-00751-4.

[19] Zhang Y, Ji X F, Gao X Z, et al. Objective-constraint mutual-guided surrogate-based particle swarm optimization for expensive constrained multi-modal problems. IEEE Transactions on Evolutionary Computation, 2023, 27(4): 908-922. DOI: 10.1109/TEVC.2022.3182810.

[20] Li G, Wang Z, Gong M. Expensive optimization via surrogate-assisted and model-free evolutionary optimization. IEEE Transactions on Systems, Man, and Cybernetics: Systems, 2023, 53(5): 2758-2769. DOI: 10.1109/TSMC.2022.3219080.

[21] Li B, Yang Y, Liu D, et al. Accelerating surrogate assisted evolutionary algorithms for expensive multi-objective optimization via explainable machine learning. Swarm and Evolutionary Computation, 2024, 88: 101610. DOI: 10.1016/j.swevo.2024.101610.

[22] Pan J S, Zhang A N, Chu S C, et al. An activity level based surrogate-assisted evolutionary algorithm for many-objective optimization. Applied Soft Computing, 2024, 164: 111967. DOI: 10.1016/j.asoc.2024.111967.

[23] He C, Zhang Y, Gong D, et al. A review of surrogate-assisted evolu-tionary algorithms for expensive optimization problems. Expert Systems with Applications, 2023, 217: 119495. DOI: 10.1016/j.eswa.2022.119495.

[24] Cai X, Zou T, Gao L. Surrogate-assisted operator-repeated evolutionary algorithm for computationally expensive multi-objective problems. Applied Soft Computing, 2023, 147: 110785. DOI: 10.1016/j.asoc.2023.110785.

[25] Chugh T, Jin Y, Miettinen K, et al. A surrogate-assisted reference vec-tor guided evolutionary algorithm for computationally expensive many-objective optimization. IEEE Transactions on Evolutionary Computation, 2018, 22(1): 129-142. DOI: 10.1109/TEVC.2016.2622301.

[26] Gu Q, Zhou Y, Li X, et al. A surrogate-assisted radial space division evolutionary algorithm for expensive many-objective optimization problems. Applied Soft Computing, 2021, 111: 107703. DOI: 10.1016/j.asoc.2021.107703.

[27] Gu Q, Zhang X, Chen L, et al. An improved bagging ensemble surrogate-assisted evolutionary algorithm for expensive many-objective optimization. Applied Intelligence: The International Journal of Artificial Intelligence, Neural Networks, and Complex Problem-Solving Technologies, 2022, 52(6): 5949-5965. DOI: 10.1007/s10489-021-02709-4.

[28] Xie L, Li G, Wang Z, et al. Surrogate-assisted evolutionary algorithm with model and infill criterion Auto-Configuration. IEEE Transactions on Evolutionary Computation, 2024, 28(4): 1114-1126. DOI: 10.1109/TEVC.2023.3291614.

[29] Zhao Y, Zeng J, Tan Y. Neighborhood samples and surrogate assisted multi-objective evolutionary algorithm for expensive many-objective optimization problems. Applied Soft Computing, 2021, 105: 107268. DOI: 10.1016/j.asoc.2021.107268.

[30] Zhen H, Gong W, Wang L. Evolutionary sampling agent for expensive problems. IEEE Transactions on Evolutionary Computation, 2023, 27(3): 716-727. DOI: 10.1109/TEVC.2022.3177605.

[31] Zhen H, Gong W, Wang L, et al. Two-stage data-driven evolutionary optimization for high-dimensional expensive problems. IEEE Transactions on Cybernetics, 2023, 53(4): 2368-2379. DOI: 10.1109/TCYB.2021.3118783.

[32] Wang W, Liu H L, Tan K C. A surrogate-assisted differential evolution algo-rithm for high-dimensional expensive optimization problems. IEEE Transactions on Cybernetics, 2023, 53(4): 2685-2697. DOI: 10.1109/TCYB.2022.3175533.

[33] Song Z, Wang H, He C, et al. A kriging-assisted two-archive evolution-ary algorithm for expensive many-objective optimization. IEEE Transactions on Evolutionary Computation, 2021, 25(6): 1013-1027. DOI: 10.1109/TEVC.2021.3073648.

[34] Wang H, Jiao L, Yao X. Two_arch2: An improved two-archive algorithm for many-objective optimization. IEEE Transactions on Evolutionary Computation, 2015, 19(4): 524-541. DOI: 10.1109/TEVC.2014.2350987.

[35] Liu Q, Jin Y, Heiderich M, et al. Surrogate-assisted evolutionary optimiza-tion of expensive many-objective irregular problems. Knowledge-Based Systems, 2022, 240: 108197. DOI: 10.1016/j.knosys.2022.108197.

[36] Liu Q, Cheng R, Jin Y, et al. Reference vector-assisted adaptive model man-agement for surrogate-assisted many-objective optimization. IEEE Transactions on Systems, Man, and Cybernetics: Systems, 2022, 52(12): 7760-7773. DOI: 10.1109/TSMC.2022.3163129.

[37] Li F, Gao L, Shen W. Surrogate-assisted multi-objective evolutionary optimization with pareto front model-based local search method. IEEE Transactions on Cybernetics, 2024, 54(1): 173-186. DOI: 10.1109/TCYB.2022.3186591.

[38] Knowles J. ParEGO: a hybrid algorithm with on-line landscape approx-imation for expensive multiobjective optimization problems. IEEE Transactions on Evolutionary Computation, 2006, 10(1): 50-66. DOI: 10.1109/TEVC.2005.851274.

[39] Liu S, Wang H, Yao W, et al. Surrogate-assisted environmental selection for fast hypervolume-based many-objective optimization. IEEE Transactions on Evolutionary Computation, 2024, 28(1): 132-146. DOI: 10.1109/TEVC.2023.3243632.

[40] Zhang J, Zhou A, Zhang G. A classification and Pareto domination based multiobjective evolutionary algorithm. In: 2015 IEEE Congress on Evolutionary Computation (CEC). Piscataway: IEEE, 2015: 2883-2890. doi; 10.1109/CEC.2015.7257247.

[41] Zhang J, Ishibuchi H, He L. A classification-assisted environmental selection strategy for multiobjective optimization. Swarm and Evolutionary Computation, 2022, 71: 101074. DOI: 10.1016/j.swevo.2022.101074.

[42] Sonoda T, Nakata M. Multiple classifiers-assisted evolutionary algorithm based on decomposition for high-dimensional multiobjective problems. IEEE Transactions on Evolutionary Computation, 2022, 26(6): 1581-1595. DOI: 10.1109/TEVC.2022.3159000.

[43] Li J, Wang P, Dong H, et al. A classification surrogate-assisted multi-objective evolutionary algorithm for expensive optimization. Knowledge-Based Systems, 2022, 242: 108416. DOI: 10.1016/j.knosys.2022.108416.

[44] Wei F F, Chen W N, Yang Q, et al. A classifier-assisted level-based learning swarm optimizer for expensive optimization. IEEE Transactions on Evolutionary Computation, 2021, 25(2): 219-233. DOI: 10.1109/TEVC.2020.3017865.

[45] Lin L, Liu T, Leng J, et al. Classification model-based assisted prese-lection and environment selection approach for evolutionary expensive bilevel optimization. Applied Intelligence, 2023, 53(23): 28377-28400. DOI: 10.1007/s10489-023-04916-7.

[46] Yuan Y, Banzhaf W. Expensive multiobjective evolutionary optimization assisted by dominance prediction. IEEE Transactions on Evolutionary Computation, 2022, 26(1): 159-173. DOI: 10.1109/TEVC.2021.3098257.

[47] Pan L, He C, Tian Y, et al. A classification-based surrogate-assisted evo-lutionary algorithm for expensive many-objective optimization. IEEE Transactions on Evolutionary Computation, 2019, 23(1): 74-88. DOI: 10.1109/TEVC.2018.2802784.

[48] He C, Tian Y, Jin Y, et al. A radial space division based evolutionary algorithm for many-objective optimization. Applied Soft Computing, 2017, 61: 603-621. DOI: 10.1016/j.asoc.2017.08.024.

[49] Zhang J, He L, Ishibuchi H. Dual fuzzy classifier-based evolutionary algorithm for expensive multiobjective optimization. IEEE Transactions on Evolutionary

Computation, 2023, 27(6): 1575 - 1589. DOI: 10.1109/TEVC.2022.3195668.

[50] Wang H, Jin Y, Doherty J. Committee-based active learning for surrogate-assisted particle swarm optimization of expensive problems. IEEE Transactions on Cybernetics, 2017, 47(9): 2664 - 2677. DOI: 10.1109/TCYB.2017.2710978.

[51] Li F, Shen W, Cai X, et al. A fast surrogate-assisted particle swarm opti-mization algorithm for computationally expensive problems. Applied Soft Computing, 2020, 92: 106303.DOI:10.1016/j.asoc.2020.106303.

[52] Zhan D, Cheng Y, Liu J. Expected improvement matrix-based infill criteria for expensive multiobjective optimization. IEEE Transactions on Evolutionary Computation, 2017, 21(6): 956 - 975. DOI: 10.1109/TEVC.2017.2697503.

[53] Zhang Q, Liu W, Tsang E, et al. Expensive multiobjective optimization by MOEA/D with Gaussian Process model. IEEE Transactions on Evolutionary Computation, 2010, 14(3): 456 - 474. DOI: 10.1109/TEVC.2009.2033671.

[54] Jones D R, Schonlau M, Welch W J. Efficient global optimization of expensive black-box functions. Journal of Global Optimization, 1998, 13(4): 455 - 492. DOI: 10.1023/A:1008306431147.

[55] Wang X, Jin Y, Schmitt S, et al. An adaptive bayesian approach to surrogate-assisted evolutionary multi-objective optimization. Information Sciences, 2020, 519: 317 - 331. DOI:.10.1016/j.ins.2020.01.048.

[56] Zhao Y, Sun C, Zeng J, et al. A surrogate-ensemble assisted expensive many-objective optimization. Knowledge-Based Systems, 2021, 211: 106520, DOI: 10.1016/j.knosys.2020.106520.

[57] Tian Y, Cheng R, Zhang X, et al. Platemo: A matlab platform for evolu-tionary multi-objective optimization. IEEE Computational Intelligence Magazine, 2017, 12(4): 73-87.DOI:10.1109/MCI.2017.2742868.

[58] Deb K, Thiele L, Laumanns M, et al (2002) Scalable multi-objective optimization test problems. In: Proceedings of the 2002 Congress on Evolutionary Computation. CEC'02 (Cat. No.02TH8600). Piscataway: IEEE, 2002: 825-830.DOI: 10.1109/CEC.2002.1007032

[59] Cheng R, Li M, Tian Y, et al. A benchmark test suite for evolutionary many-objective optimization. Complex & Intelligent Systems, 2017, 3: 67-81.DOI:10.1007/s40747-017-0039-7.

[60] Zhou A, Jin Y, Zhang Q, et al. Combining model-based and genetics-based offspring generation for multi-objective optimization using a convergence criterion. In: 2006 IEEE International Conference on Evolutionary Computation. Piscataway: IEEE, 2006: 892 - 899. DOI: 10.1109/CEC.2006.1688406.

[61] Zhang Q, Zhou A, Jin Y. RM-MEDA: A regularity model-based multiob-jective estimation of distribution algorithm. IEEE Transactions on Evolutionary Computation, 2008, 12(1): 41 - 63. DOI: 10.1109/TEVC.2007.894202.